Rock-magnetic and paleomagnetic results from the Tepic-Zacoalco rift region (western Mexico)

MANUEL CALVO-RATHERT[1], BERTHA AGUILAR REYES[2], AVTO GOGUITCHAICHVILI[2,1], JOSÉ ROSAS ELGUERA[3], HÉCTOR FRANCO[2], JUAN MORALES[2], RUTH SOTO[4], ÁNGEL CARRANCHO[1,5] AND HUGO DELGADO[6]

1 Departamento de Física, Escuela Politécnica Superior, Universidad de Burgos, c/ Francisco de Vitoria, s/n, 09006 Burgos, Spain (mcalvo@ubu.es)

2 Laboratorio Interinstitucional de Magnetismo Natural, Instituto de Geofísica - Unidad Michoacán, UNAM-Campus Morelia, Mexico

3 Universidad de Guadalajara, CUCEI, Mexico

4 Instituto Geológico y Minero de España, c/ Manuel Lasala 44, 50006 Zaragoza, Spain

5 Centro Nacional de la Investigación en Evolución Humana, Av. De la Sierra de Atapuerca,s/n, 09002 Burgos, Spain

6 Departamento de Vulcanología, Instituto de Geofísica, UNAM, Ciudad Universitaria, 04510 México, DF.

Received: May 16, 2012; Revised: October 11, 2012; Accepted: January 2, 2013

ABSTRACT

A rock-magnetic and paleomagnetic investigation was carried out on eleven Pleistocene and Pliocene $^{40}Ar/^{39}Ar$ dated lava flows from the Tepic-Zacoalco rift region in the western sector of the Trans-Mexican Volcanic Belt (TMVB) with the aim of obtaining new paleomagnetic data from the study region and information about the Earth's magnetic field recorded in these rocks. Rock-magnetic experiments including measurement of thermomagnetic curves, hysteresis parameters and isothermal remanence acquisition curves were carried out to find out the carriers of remanent magnetisation and to determine their domain structure. Although some samples were characterised by the presence of a single ferromagnetic phase (magnetite), in most cases more phases were observed. Analysis of hysteresis parameters showed a mixture of single domain and multidomain particles, the fraction of the latter varying between 40% and 80%. Paleomagnetic results were obtained in all sites, although in 7 sites characteristic remanence directions and remagnetisation circles had to be combined in order to calculate site means. The six Pliocene sites not showing intermediate polarity yielded a paleomagnetic pole (latitude $\phi = 81.1°$, longitude $\lambda = 94.3°$) which roughly agrees with the expected one. Paleomagnetic directions do not indicate significant vertical-axis block rotations in the western TMVB area. Reversed polarities observed can be correlated to the Gilbert chron, normal polarities to the Gauss chron or the Brunhes chron and intermediate polarities to the Cochiti-Gilbert or the Gilbert-Gauss transition. The reversed or intermediate polarity magnetisation recorded in one of the sites (542 ± 24 ka) corresponds either to the West Eifel 4 or the West Eifel 5 excursion, while the reversed

© 2013 Inst. Geophys. AS CR, Prague

polarity observed in the other site (220 ± 36 ka) very likely provides new evidence for the Pringle Falls excursion or the event recorded in the Mamaku ignimbrite.

Keywords: paleomagnetism, rock magnetism, Trans-Mexican Volcanic Belt, geomagnetic excursion

1. INTRODUCTION

The Earth's magnetic field is not static, as its direction and strength vary with time. According to their magnitude, length and global or regional character, different types of variations can be distinguished. In fact, one of the main characteristics of the Earth's magnetic field is that it switches its polarity. The duration of geomagnetic polarity intervals is rather variable, ranging between some tens of thousands and several millions of years. The term polarity chrons is used for the main subdivisions of time recognised on the basis of polarity, while short (0.1 Ma) polarity intervals occurring within a chron are termed subchrons (*Harland et al., 1990*). Periods of stable polarity are interrupted in several occasions by short-lived geomagnetic "events" of a few thousands of years of duration (e.g., *Laj and Channell, 2007*). *Cande and Kent (1992a, b)* called cryptochrons those "events" with a duration of less than 30 ka, but terminology based on duration of polarity intervals can be problematic in these cases: Although some cryptochrons could be described as short-lived polarity intervals and others as aborted reversals or geomagnetic excursions, paleomagnetic records are always compromised by limitations of the recording medium and the availability of chronological tools of adequate precision. *Laj and Channell (2007)* therefore propose using the term microchron for brief polarity chrons with established duration of less than 10^5 years and the term excursion for features that represent departures from normal secular variation, for which full polarity reversal has not been proved. *Singer et al. (2002)* proposed the development of a Geomagnetic Instability Time Scale (GITS), as they considered that in order to analyse the degree of stability of the geodynamo not only the undisputed polarity reversals, but also the short-lived geomagnetic "events" had to be taken into account. In the last few decades numerous geomagnetic excursions have been discovered in the previously believed stable Brunhes chron (e.g., *Singer et al., 2002*; *Laj and Channell, 2007*). All the excursions recognised in the Bruhnes chron are relatively brief geomagnetic instabilities characterised by a decrease in intensity associated with a large directional shift from the dipolar field direction (larger than secular variation), immediately followed by a return to the state previous to the excursion (e.g., *Laj and Channell, 2007*). The number of excursions recorded in the Brunhes chron is, however, still a matter of debate, as besides some well established ones like the Laschamp excursion, other are still poorly documented. *Laj and Channell (2007)*, for instance, consider that in the Brunhes chron only seven adequately defined excursions with acceptable age control can be found, whereas other five ones still need further ratification either in definition of magnetic data or in refinement of the age models.

Sedimentary rocks are able to provide continuous magnetisation records, thus supplying an uninterrupted register of geomagnetic field variations. Even so, and although most estimates of the duration of field transitions have been derived from sediments, the

specific characteristics of remanent magnetisation of sedimentary rocks - depositional (*DRM*) or postdepositional (*pDRM*) remanent magnetisation - can hamper obtaining a faithful field variation record. Volcanic rocks, on the other hand, allow a reliable and instantaneous record of the Earth's magnetic field by means of the acquisition of thermoremanent magnetisation (*TRM*), although being tied to volcanic eruptions, they provide a discontinuous record. Nevertheless, because volcanic rocks are in principle able to offer a more faithful though instantaneous image of the Earth's magnetic field, the paleomagnetic study of lava flows can be of major interest for the knowledge of characteristics and variations of the ancient geomagnetic field. In order to be useful, this kind of paleomagnetic studies needs to be supplemented by precise rock-age data, as the usefulness of GITS studies on volcanic rocks is rather limited when the age of the studied units is poorly constrained.

In the present study we report a rock-magnetic and paleomagnetic investigation carried out on 11 independent Pleistocene and Pliocene lava flows from the Tepic-Zacoalco rift region in the western sector of the Trans-Mexican Volcanic Belt (TMVB) with the aim of obtaining new paleomagnetic data from the study region. Precise new rock-age data are available for all studied sites, as they have recently been dated by means of the $^{40}Ar/^{39}Ar$ method by *Frey et al. (2007)* and *Frey et al. (submitted to Bull. Volcanol.)*. Combination of both new paleomagnetic and radiosiotopic data obtained in the same units can provide interesting information about the Earth's magnetic field recorded in these Quaternary and Pliocene rocks.

2. GEOLOGICAL SETTING, PREVIOUS PALEOMAGNETIC STUDIES, $^{40}Ar/^{39}Ar$ AGES AND SAMPLING

The Trans-Mexican Volcanic Belt is a continental magmatic arc located in the southern margin of the North American plate (Fig. 1a). It extends approximately 1000 km across Mexico from the Pacific to the Gulf of Mexico with a W-E trend and has a variable width of 65–200 km. The TMVB is composed of stratovolcanoes, cinder cone fields and silicic caldera complexes, and volcanic activity is related to the subduction of the Rivera and Cocos plates beneath southern Mexico along the Middle American trench.

The TMVB can be divided into three major structural units (*Pasquaré et al., 1988*; *Alaniz-Álvarez et al., 1998*), which are characterised by different tectonic styles, geochemical composition and volcanic activity: The Western, Central and Eastern sectors. The present study was carried out on rocks from the region of the Tepic-Zacoalco rift, a NW-trending corridor that is approximately 50 km wide and extends from the Pacific coast to south of the city of Guadalajara (Fig. 1a,b) and is located in the Western sector of the TMVB. The Tepic-Zacoalco rift is part of a triple rift system and defines the northern boundary of the Jalisco block (Fig. 1b). The predominant basement rock-types in the Tepic-Zacoalco rift are rhyolitic ash-flow tuffs and lavas.

A relatively large amount of radiometric data is available for this area. *Frey et al. (2007)* performed $^{40}Ar/^{39}Ar$ age determinations on 32 volcanic samples from the Tepic-Zacoalco rift as well as on 6 dike samples from the interior of the Jalisco block and 3 dikes from the NW margin of the Tepic-Zacoalco rift, obtaining ages ranging between 289 ka and 48.8 Ma for the volcanic samples and between 11.00 and 73.10 Ma for the

dikes, Cretaceous ages being observed only in the six dikes from the Jalisco bloc. A summary of results and references corresponding to previous K/Ar and $^{40}Ar/^{39}Ar$ age determinations in the study area is provided by *Frey et al. (2007)*, with results ranging between 1.50 and 91.5 Ma. Additional $^{40}Ar/^{39}Ar$ data from this region are provided by a new study carried out by *Frey et al. (submitted to Bull. Volcanol.)* in the Tepeltitic volcano area, which yields ages between 185 and 575 ka.

A few paleomagnetic studies have already been carried out on samples belonging to the western sector of the TMVB. *Ruiz-Martínez et al. (2010)* performed a paleomagnetic study on 11 sites from the western and 40 sites from the central sectors of the TMVB of Quaternary, Pliocene and Miocene age, obtaining 9 mean site directions in the former and 38 in the latter. Paleomagnetic results indicate no paleomagnetically detectable vertical-axis block rotations in the study areas. *Rosas-Elguera et al. (2011)* performed a paleomagnetic study on 16 Eocene andesitic dikes from the Tecalitlan area, which is

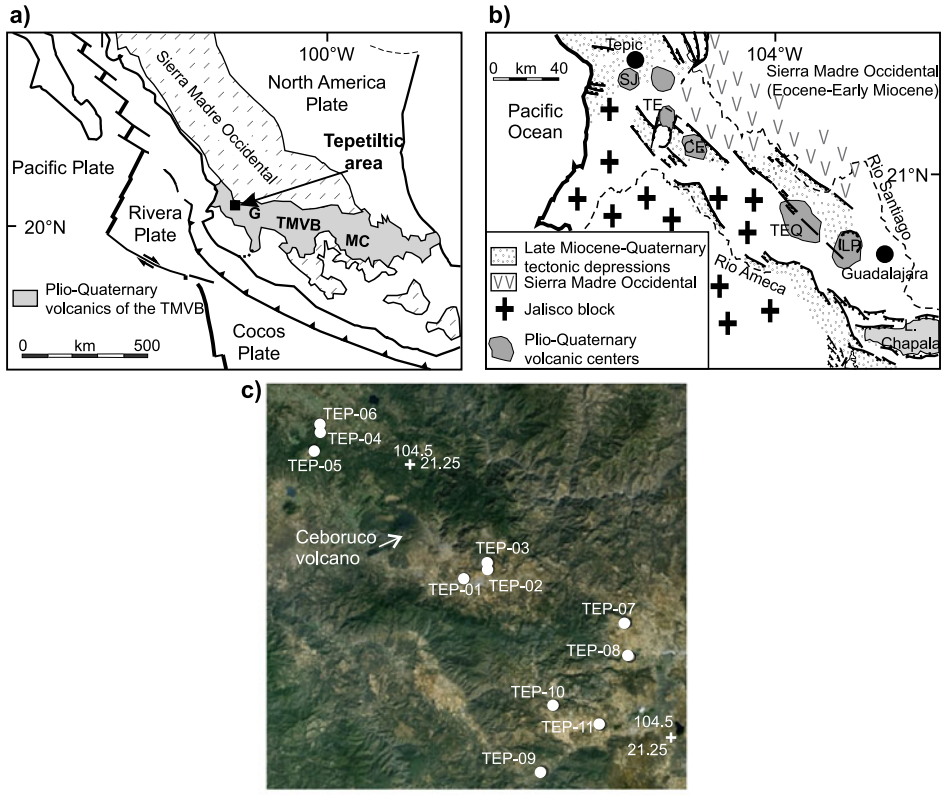

Fig. 1. **a)** Schematic geological map of the Trans-Mexican Volcanic Belt (TMVB). The black square shows the Tepeltitic area, in which sampling was performed. G: Guadalajara; MC: Mesa Central. Inset highlights the Tepic-Zacoalco rift region. **b)** Schematic geological map of the Tepic-Zacoalco rift region. SJ: San Juan volcano; TE: Tepeltitic volcano; CE: Ceboruco volcano; TEQ: Tequila volcano; LP: La Primavera caldera. **c)** Location of sampling localities in the Tepeltitic area.

Table 1. Description of studied sites.

Flow	Composition	Age [Ma]	Lat. [°N]	Long. [°E]
TEP6	Basaltic andesite	0.220 ± 0.036	21.3261	255.2660
TEP5	Rhyolite	0.307 ± 0.034	21.2803	255.3166
TEP4	Basaltic andesite	0.542 ± 0.024	21.2548	255.3060
TEP11	Ryolithic flow	2.91 ± 0.03	20.7723	255.8617
TEP10	Ryolithic flow	3.30 ± 0.01	20.8163	255.7735
TEP7	Ryolithic flow	3.40 ± 0.04	20.9635	255.9137
TEP8	Rhyolitic flow	3.54 ± 0.01	20.9018	255.9203
TEP3	Basaltic flow	3.87 ± 0.04	21.0623	255.6500
TEP9	Andesite	3.99 ± 0.05	20.6967	255.7497
TEP1	Basalt	4.01 ± 0.02	21.0463	255.6037
TEP2	Rhyolite	4.32 ± 0.01	21.0733	255.6507

located in the Michoacán block, carrying out a $^{40}Ar/^{39}Ar$ on one of the dikes, which yielded an age of (35.0 ± 1.8) Ma. The mean declination observed in this study did not disagree significantly from the expected one and thus did not indicate vertical-axis block rotations. *Petronille et al. (2005)* studied 17 independent lava flows collected in the Ceboruco-San Pedro volcanic field, with $^{40}Ar/^{39}Ar$ ages ranging from 2 to 819 ka. They found two reversed polarity flows, which they ascribed to the Big Lost excursion and an intermediate polarity flow which they interpreted as recording the Matuyama-Brunhes precursor. *Rodríguez-Ceja et al. (2006)* investigated 24 independent cooling units in the Tequila area, with $^{40}Ar/^{39}Ar$ ages ranging from 150 to 1130 ka. Paleomagnetic results showed the presence of an intermediate polarity flow recording the Delta excursion and two reversed polarity flows which were interpreted as possibly recording the Levantine excursion at approximately 360 ka.

Sampling strategy was conditioned by $^{40}Ar/^{39}Ar$ data from *Frey et al. (2007)* and *Frey et al. (submitted to Bull. Volcanol.)*, as only sites with available radioisotopic dates from those studies were sampled. Samples were taken from three sites of Pleistocene age and eight sites of Pliocene age (Fig. 1c). 102 cores from 11 independent cooling units (8–10 cores per flow) were sampled with a gasoline-powered portable drill and oriented with both a magnetic and a sun compass. The sampled sites consisted of rhyolithic, basaltic or andesitic flows. No bedding correction had to be applied. Table 1 shows location, ages and composition of the 11 sampling sites.

3. ROCK-MAGNETIC EXPERIMENTS

Rock-magnetic experiments were carried out to find out the carriers of remanent magnetisation and to determine their domain structure. They included the measurement of thermomagnetic curves - strong-field magnetisation versus temperature (J_S-T) and susceptibility versus temperature (κ-T) curves, hysteresis parameters and isothermal remanent magnetisation (IRM) acquisition curves.

Most of the rock-magnetic experiments were performed with a Variable Field Translation Balance (VFTB) in the University of Burgos (Spain). For these measurements a whole-rock powdered sample was taken from each flow (two samples in site TEP8 and none from TEP9) and subjected to the following measurement sequence: (i) IRM acquisition, (ii) backfield, (iii) hysteresis curve and (iv) J_S-T curve. κ-T curves were mostly recorded with a Bartington Kappa-bridge in the paleomagnetic laboratory of the Universidad Nacional Autónoma de México in Morelia (Mexico). For this kind of measurements a single whole-rock powdered sample was chosen from each flow (two samples in site TEP9) to be heated in air to a maximum temperature between 600 and 700°C and cooled down to room temperature. κ-T curves of samples from flows TEP2 and TEP8, however, were measured with a CS3 furnace attached to a KLY4 susceptibility bridge at heating and cooling rates of 10°C min^{-1}, in the paleomagnetic laboratory of the University of Burgos (Spain). Also in this case a single whole-rock powdered sample was chosen from each flow to be heated in air to a peak temperature of 700°C and cooled down to room temperature. No κ-T curve was measured for site TEP11.

Curie temperatures T_C from the J_S-T curves were determined using the two-tangent method (*Grommé et al., 1969*). On the other hand, Curie points from the κ-T curves were determined taking inflexion points in the curves following the drop of susceptibility corresponding to the destruction of ferromagnetic phases (*Prévot et al., 1983*), as application of the two-tangent method can produce an overestimation of the Curie temperature (*Petrovský and Kapička, 2006*). Thermomagnetic behaviour observed with both methods is rather similar and Curie temperatures determined show a reasonable agreement although they are not equal (Table 2). It should be taken into account, however, that different samples were taken in each flow for κ-T and J_S-T experiments.

The simplest thermomagnetic behaviour was observed in sites TEP1, TEP3, TEP8 and TEP10. As will be discussed below, site TEP1 also exhibits a simple paleomagnetic behaviour. In these sites, heating and cooling curves from both κ-T and J_S-T experiments show a single ferromagnetic (s.l.) phase (Fig. 2a), although in both measured TEP8 J_S-T cooling curves a weak high-temperature phase (T_C = 646°C) can be recognised (Table 2, Fig. 2b). Only both thermomagnetic curves from TEP1 and J_S-T curve of TEP3 display a nearly reversible behaviour (Fig. 2a), in all other thermomagnetic curves recorded in these sites, magnetisation and susceptibility values of the cooling curves are clearly weaker than those of the heating curves. Curie temperatures observed in this group of sites, besides the already mentioned weak high-temperature phase in TEP8, lie in all other cases in a 513 to 595°C range, which can be ascribed to the presence of low-Ti titanomagnetite or Al or Mg substituted magnetite. It can be observed, however, that in all cases Curie temperatures determined from the heating curve are higher than those determined from the cooling curve (Table 2). The difference is higher in κ-T than in J_S-T curves. Although a part of this disagreement can be ascribed to a difference between the recorded and the real specimen temperature, we do not think that this effect is the main reason of the observed discrepancy. In κ-T experiments, where a greater difference between Curie points was observed between heating and cooling curves, the temperature increase and decrease rate was set at 10°C per minute and the specimen was powdered,

Table 2. Rock-magnetic results. *SIRM* - saturation isothermal remanent magnetisation; M_{RS}/M_S - remanent saturation to induced saturation magnetisation ratio; B_{CR}/B_C - coercivity of remanence to coercivity ratio; B_{RH}/B_{CR} - ratio of coercivity ratio and coercivity of remanence (see text); Shape - hysteresis curve shape parameter. An asterisk indicates mean values obtained from two specimens from the same site. T_{C1}, T_{C2}, T_{C3} - Curie temperatures obtained from the heating and cooling curves of magnetisation-versus-temperature (J_S-T) and susceptibility-versus-temperature (κ-T) experiments. In brackets - Curie temperatures of weak not easily distinguishable phases. J_S-T and κ-T curves from the same site were obtained on different specimens.

Site	*SIRM* [Am^2kg^{-1}]	M_{RS}/M_S	B_{CR}/B_C	B_{RH}/B_{CR}	Shape	J_S-T					κ-T			
						Heating		Cooling			Heating		Cooling	
						T_{C1} [°C]	T_{C2} [°C]	T_{C1} [°C]	T_{C2} [°C]	T_{C3} [°C]	T_{C1} [°C]	T_{C2} [°C]	T_{C1} [°C]	T_{C2} [°C]
TEP1	8.57×10^{-2}	0.12	2.57	2.04	–0.86	571		543			576		513	
TEP2	3.22×10^{-3}	0.30	2.86	1.46	0.63	592	(228)	567	231	(665)				
TEP3	6.60×10^{-2}	0.14	2.68	0.70	–0.71	571		546			568		529	
TEP4	1.08×10^{-2}	0.11	3.33	1.95	–0.74	595	(410)	579	434	(637)	611	354	579	338
TEP5	9.35×10^{-2}	0.17	2.55	1.88	–0.68	581		553	361		549		549	150
TEP6	1.07×10^{-1}	0.23	1.97	1.42	–0.70	574	189	536			575	142	537	
TEP7	2.39×10^{-2}	0.26	1.98	1.34	–0.75	595	457	571		(665)	613	373	576	
TEP8	5.45×10^{-3}*	0.11*	3.98*	2.01*	–0.60*	553/578		551/537		(665/660)				---/285
TEP9											592/550	278/---	563/537	
TEP10	1.32×10^{-2}	0.23	2.03	1.24	–0.66	585		574		(665)	591		551	
TEP11	2.69×10^{-3}	0.22	1.92		–0.93	585	250	553						

thus having a large effective surface for heating and cooling. The higher Curie temperatures of the heating curves (in TEP10 T_C = 595°C, above the Curie temperature of magnetite) and the lower Curie temperatures of the cooling curves, together with the presence of a weak high Curie temperature (646°C) phase in TEP8 point to (slightly maghemitised) magnetite as the carrier of remanence. This would be in accordance with the weaker susceptibilities and magnetisations observed in the cooling curves, pointing towards an inversion of the (substituted) magnetite-maghemite solid solution to a hematite-magnetite intergrowth.

Thermomagnetic behaviour of the remaining sites is more complex and all curves show an irreversible behaviour. In all heating curves a ferromagnetic (s.l.) phase is

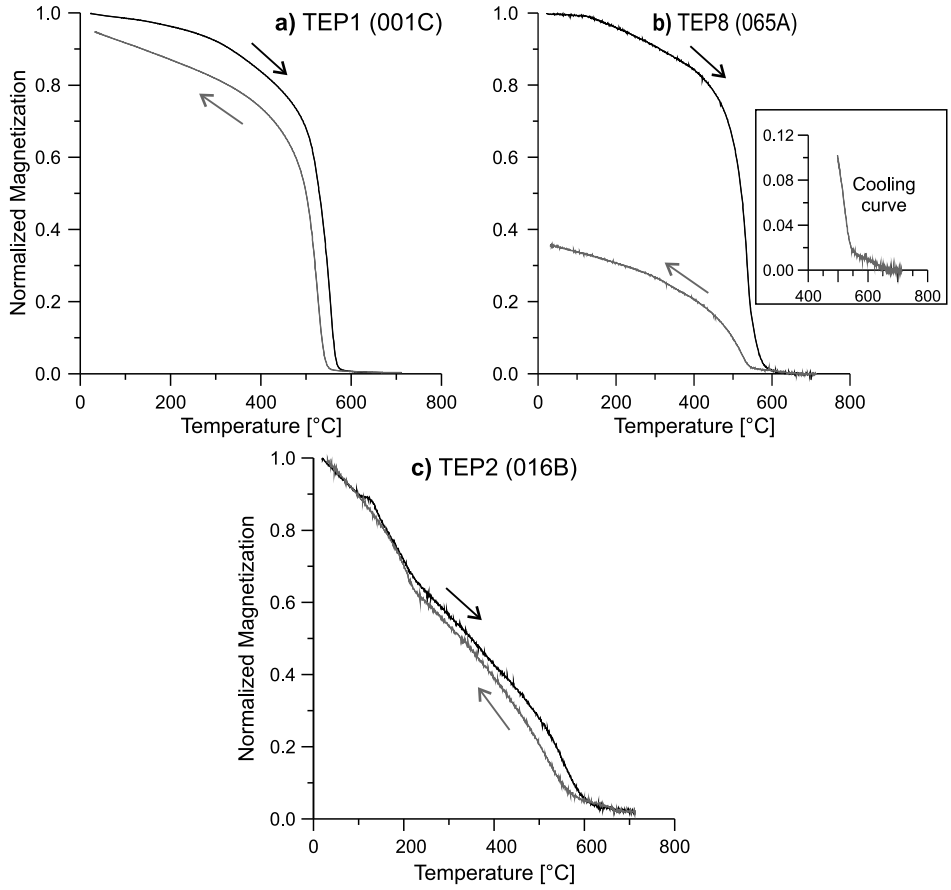

Fig. 2. Normalized strong field magnetisation-versus-temperature curves from lava flow samples from the Tepeltitic area. **a)** Example of a single-phase nearly reversible curve (sample 001C, site TEP1). **b)** Example of an irreversible curve (sample 065C, site TEP8). A weak high-temperature phase can be observed in the cooling curve (inset). **c)** Example of a nearly reversible curve with two ferromagnetic (s.l.) phases of high and low Curie temperature (sample 016B, site TEP2).

observed which has Curie temperatures in a 549 to 595°C range, which as in the previously discussed cases can be ascribed to the presence of low-Ti titanomagnetite or Al or Mg substituted magnetite in the case of the lower Curie temperatures and to the presence of (slightly maghemitised) magnetite as the carrier of remanence of remanence in the case of Curie temperature values exceeding the Curie point of magnetite. In addition, another phase with low or intermediate Curie temperatures (142 to 457°C) can be recognised in the heating curves of both κ-T and J_S-T experiments of most of these sites, although in some cases it is difficult to distinguish (Table 2, in brackets). In site TEP5, this low/intermediate T_C phase in the heating curve is absent. If cooling curves are analysed, a near-magnetite phase can be observed in all of them and like in the initially discussed simpler thermomagnetic curves, their Curie temperatures are in almost all cases lower than those of the heating curves. In addition, a phase with low or intermediate Curie points is observed in a few cases. Besides that, in J_S-T curves of sites TEP4 and TEP7 a weak high-temperature phase ($T_C > 637$°C) can be detected (Table 2). During heating, inversion of the (substituted) magnetite-maghemite solid solution to a hematite-magnetite intergrowth might occur. The decrease in Curie temperature and magnetisation/susceptibility could also be interpreted as due to temperature-induced Ti diffusion which leads to an increased Ti-content in the Ti-poor titanomagnetite (*Soffel, 1975*), specially in those cases in which no high-temperature phase is found in the cooling curve. Thermally stable intermediate and low Curie-temperature phases are probably related to the presence of either titanomagnetite with $x = 0.2$ to 0.6 degree of Ti substitution or titanohematite. Thermally unstable phases in this Curie-temperature range could also be titanomaghemites.

J_S-T curve of site TEP2 (Fig. 2c) deserves to be especially mentioned. This apparently almost fully reversible curve shows a stable low Curie temperature as well as a "near magnetite" Curie point both in the heating and the cooling curve. The latter Curie point is, however, 25°C higher in the heating than in the cooling curve. A closer look at the cooling curve shows the presence of a weak high-temperature Curie point. Information from the isothermal remanent magnetisation acquisition curve of site TEP2 (Fig. 3b) suggests that the low Curie-temperature phase is high-coercivity antiferromagnetic titanohematite, which is still in accordance with its determined Curie temperature of approximately 230°C, corresponding to a degree of titanium substitution near $y = 0.45$ threshold which separates antiferromagnetic and ferromagnetic behaviour of titanohematites (e.g., *Dunlop and Özdemir, 1997*).

Isothermal remanent magnetisation (IRM) acquisition curves were recorded in a maximum applied field of approximately 1 T. Low-coercivity phases appear to be the main carriers of remanence, as could be seen in samples from sites TEP1, TEP3, TEP4 and TEP6, where saturation is reached at applied fields below 190 mT (Table 2), and in samples from sites TEP5, TEP7, TEP8, TEP10 and TEP11, in which an applied field of 190 mT is capable to achieve approximately 85 to 95% of the saturation value (Fig. 3a). In some cases saturation is not completely attained, pointing to the presence a small contribution of a high-coercivity phase. On the other hand, IRM acquisition curve of site TEP2 is dominated by a high-coercivity phase (Fig. 3b). At low applied fields below 70 mT a low-coercivity phase can be recognised, but application of higher fields clearly changes the slope of the IRM acquisition curve which does not reach saturation at an

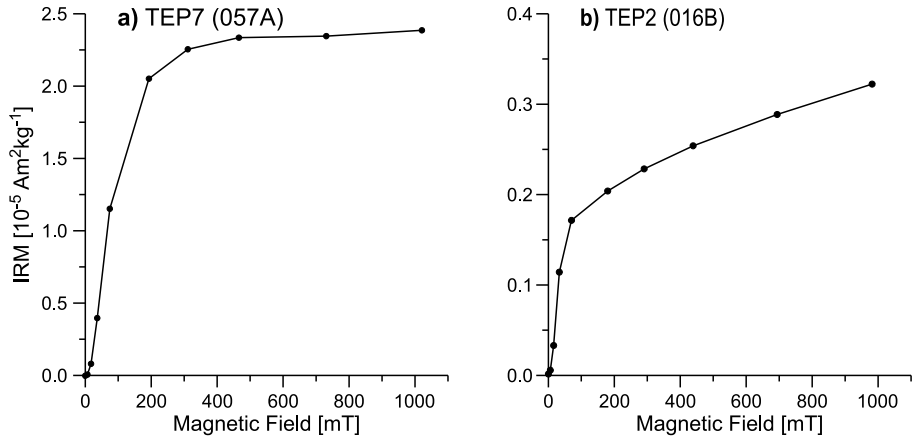

Fig. 3. Isothermal remanent magnetisation acquisition curves. **a)** Example of a sample with low-coercivity phase as main carrier of remanence (sample 057A, site TEP7); **b)** example of a sample showing the presence of a strong high-coercivity phase (sample 016B, site TEP2).

applied field of 1 T. The low coercivity phase only makes up approximately 50% of the IRM value attained at 1 T.

Hysteresis parameters were obtained from hysteresis and backfield curves and the RockMagAnalyzer 1.0 software (*Leonhardt, 2006*) was used to analyse the measured curves. Fig. 4 shows the determined hysteresis parameters. As suggested by this figure and Table 2, the grain size of the studied samples plots mainly in the PSD (pseudo-single-domain) area (*Day et al., 1977*). This behaviour might be also explained by a mixture of single-domain (SD) and multi-domain (MD) particles (*Dunlop, 2002*), the proximity to the saturation remanence to saturation magnetisation ratio (J_{RS}/J_S) of 0.02 (PSD-MD region boundary, *Dunlop, 2002*) shown in the figure indicating an increasing amount of the MD component. If the data from the present study are compared with theoretical Day plot curves calculated for magnetite (*Dunlop, 2002*), their relative amount of MD particles in the mixture would vary between approximately 40% (TEP6, TEP7, TEP10 and TEP11) and 80% (TEP4 and both TEP8 samples), with samples TEP1, TEP3 and TEP5 corresponding to a 60% MD composition. Sample TEP2, which carries high-coercivity antiferromagnetic titanohematite together with magnetite, plots in a different sector of the Day diagram.

Though useful, information provided by Day-plots can be often ambiguous. High J_{RS}/J_S ratios are indicative of the presence of SD or PSD grains as remanence carriers. Low J_{RS}/J_S ratios, however, can be observed both if large MD particles or small superparamagnetic (SP) particles are abundant. Shape parameter σ_{HYS} and coercivity ratio B_{RH}/B_{CR} (*Fabian, 2003*) may provide some additional information about the domain state of the studied samples. Graphically B_{RH} is the positive field value where the difference between upper and lower hysteresis branches has decreased from $2\,J_{RS}$ to J_{RS} at $B = 0$. High B_{RH}/B_{CR} ratios indicate large particles, while B_{RH}/B_{CR} ratios below 1 are observed

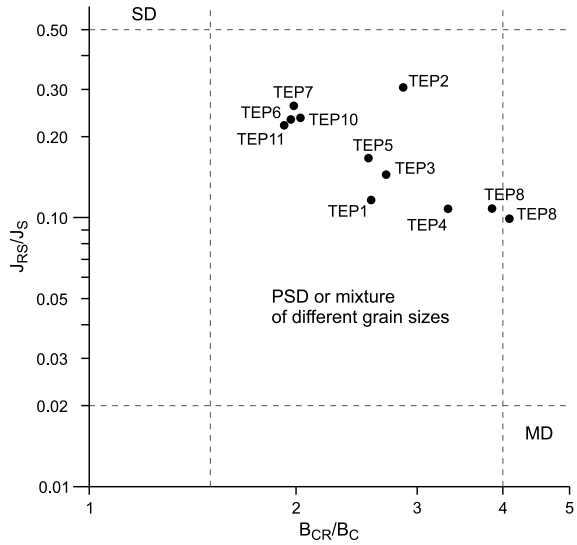

Fig. 4. Bi-logarithmic Day-plot (*Day et al., 1977*) modified after *Dunlop (2002)*. J_{RS}/J_S - saturation remanence to saturation magnetisation; B_{CR}/B_C - coercivity of remanence to coercivity.

in natural ensembles containing SP particles (*Fabian, 2003*). Shape anomalies of hysteresis loops are often interpreted as being indicative of mixtures of fractions with highly contrasting coercivities (e.g., *Roberts et al., 1995*; *Muttoni, 1995*) originating from mixed assemblages of multiple magnetic components with different mineralogy or grain size. The shape parameter σ_{HYS} gives a quantitative measure related to the shape of the hysteresis loop, with $\sigma_{HYS} > 0$ for wasp-waisted loops and $\sigma_{HYS} < 0$ for pot-bellied loops. This parameter is relatively independent of grain size within the SD-MD region, so that variations in σ_{HYS} are indicative of the presence of SD grains or other mineral fractions (*Fabian, 2003*).

Shape parameter σ_{HYS} was observed to be negative in all but one case (TEP2), indicating pot-bellied hysteresis curves. Fig. 5 shows a plot of the latter parameter versus B_{RH}/B_{CR} ratio. The variation of σ_{HYS} is relatively low, so that the larger differences observed in the B_{RH}/B_{CR} ratio among the analysed samples can be mainly ascribed to their SD-MD trend, perhaps with the exception of site TEP3, where a $B_{RH}/B_{CR} < 1$ may signal the presence of SP particles.

4. PALEOMAGNETIC MEASUREMENTS

Paleomagnetic measurements were performed at the paleomagnetic laboratory of the Universidad Nacional Autónoma de México in Morelia (Mexico). In each one of the studied 11 sites, a pilot sample was subjected to thermal and another pilot sample to alternating field (AF) demagnetisation. Analysis of demagnetisation results allowed

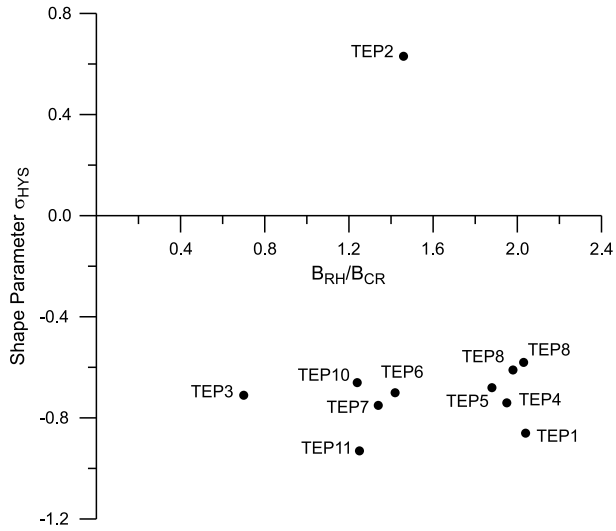

Fig. 5. Plot of shape parameter σ_{HYS} versus B_{RH}/B_{CR}. B_{RH} - coercivity ratio (see text); B_{CR} - coercivity of remanence.

choosing the most suitable demagnetisation technique, so that 6 to 11 specimens from all 11 studied sites were finally subjected either to stepwise thermal or AF demagnetisation. Remanent magnetisation was measured with a JR5 spinner magnetometer, thermal demagnetisation was performed with a MMDT (Magnetic Measurements Ltd.) furnace and AF demagnetisation with a GSD-5 degausser (Schonstedt). Directions of remanent magnetisation components were determined in all cases by means of principal component analysis (*Kirschvink, 1980*).

Mean *NRM* directions, which are shown in Table 3, are characterised by a large scatter, except in sites TEP1, TEP7 and TEP9. Demagnetisation characteristics during paleomagnetic treatment varied depending on the site analysed. The simplest behaviour could be observed in sites TEP1, TEP7 and TEP9, in which only a single paleomagnetic component, often accompanied by a small secondary component could be detected (Fig. 6a) which could be easily erased at maximum temperatures of 200°C or maximum fields of 20 mT. Characteristic remanence (*ChRM*) in site TEP7 displays a normal polarity, while sites TEP1 and TEP9 yield reverse polarity directions (Table 3). As previously mentioned, site TEP1 also displays the simplest κ-T curve.

Paleomagnetic analysis of sites TEP4 and TEP10 was less straightforward. In these sites, single-component samples coexist with samples in which a sometimes weak and sometimes rather strong viscous initial component appears together with the characteristic component (Fig. 6c). In some cases, overlapping of both components and failure of complete AF-demagnetisation hinders direct determination of the characteristic component. In these cases we determined remagnetisation circles, as they were much better defined than *ChRM* directions and chose to combine directions of better quality with remagnetisation circles (*McFadden and McElhinny, 1988*) (Table 3).

Table 3. Paleomagnetic results. *NRM* - natural remanent magnetisation; *ChRM* - characteristic remanent magnetisation; *N* - number of specimens used for *NRM* determination; *N* (*D* + *P*) - number of cores used for *ChRM* determination. In brackets - the number of directly determined directions (*D*) and planes (*P*); *n/r* - number of specimens used (*n*) and rejected (*r*) for *ChRM* determination; *Dec.* - declination. *Inc.* - inclination; α_{95} - radius of 95% confidence cone; *k* - precision parameter. *PLat.* - VGP Latitude (North). *PLong.* - VGP Longitude (East); Pol. - polarity (N - normal, R - reversed, I - intermediate).

Site	Age [Ma]	*NRM*					*ChRM*						*Plat.* [°N]	*PLong.* [°E]	Pol.
		N	Dec. [°]	Inc. [°]	k	α_{95} [°]	*N* (*D* + *P*)	*n/r*	Dec. [°]	Inc. [°]	k	α_{95} [°]			
TEP6	0.220 ± 0.036	9	441.1	–5.7	3.5	32.4	7 (3 + 4)	8/1	148.2	–26.5	21.0	14.3	–58.9	337.0	R
TEP5	0.307 ± 0.034	8	9.3	15.6	2.1	51.9	7 (4 + 3)	11/2	338.5	50.6	257.8	3.9	68.3	197.4	N
TEP4	0.542 ± 0.024	7	73.6	–31.2	3.5	37.8	5 (2 + 3)	8/2	135.9	–40.7	86.1	9.4	–49.3	356.7	I/R
TEP11	2.91 ± 0.03	11	58.5	15.0	5.2	22.1	9 (1 + 8)	9/0	358.3	19.9	180.1	4.3	79.4	85.0	N
TEP10	3.30 ± 0.01	10	26.8	50.4	5.5	22.6	7 (6 + 1)	7/0	3.5	34.5	172.6	4.7	86.2	14.5	N
TEP7	3.40 ± 0.04	10	346.7	34.9	58.6	10.9	8 (8 + 0)	8/0	345.1	36.1	50.2	7.9	74.5	165.4	N
TEP8	3.54 ± 0.01	8	327.7	12.2	2.1	52.1	8 (2 + 6)	8/0	237.3	–41.8	36.2	10.1	–37.3	151.0	I
TEP3	3.87 ± 0.04	10	172.4	–4.9	12.0	14.6	10 (10 + 0)	11/0	179.3	–15.5	27.8	9.3	–76.8	258.7	R
TEP9	3.99 ± 0.05	10	185.8	–24.0	115.5	4.5	8 (8 + 0)	8/0	180.8	–25.2	121.8	5.0	–82.5	249.8	R
TEP1	4.01 ± 0.02	8	176.6	1.5	58.8	7.3	6 (6 + 0)	6/0	176.7	–6.9	263.7	4.1	–72.1	266.4	R
TEP2	4.32 ± 0.01	8	296.9	–30.1	2.9	40.2	6 (1 + 5)	9/0	38.1	–55.4	32.2	14.2	22.6	42.9	I

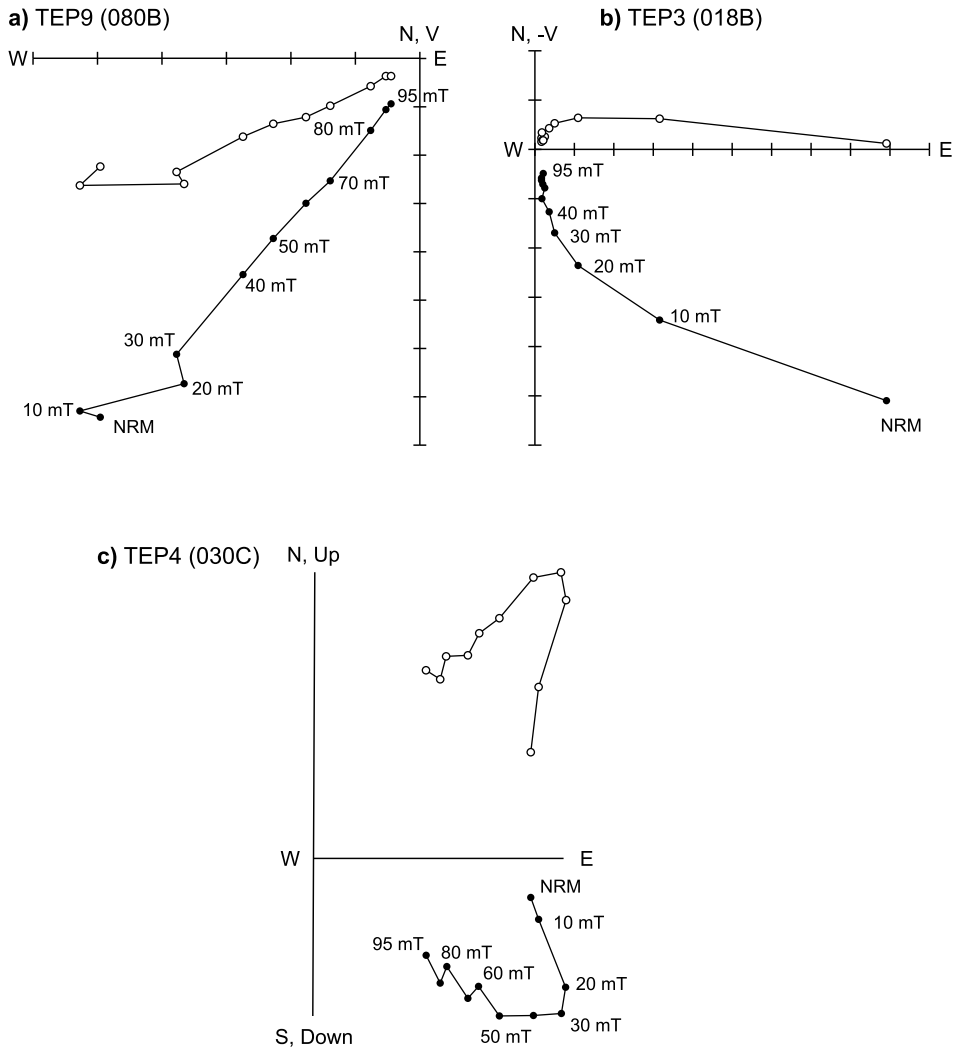

Fig. 6. Orthogonal demagnetisation vector plots. **a)** AF demagnetisation of 080B (TEP9); **b)** thermal demagnetisation of 018B (TEP3); **c)** AF demagnetisation of 030C (TEP4). Solid symbols are for the horizontal projections and open symbols for the vertical projections.

In sites TEP2 and TEP3 most specimens are characterised by the presence of two more or less overlapped components (Fig. 6b). However, while in the latter site *ChRM* can be easily isolated and directions calculated, in TEP2 overlapping hinders in most cases direct determination of the characteristic component and remagnetisation circles had to be determined in most specimens. Mean direction of TEP2 was obtained combining remagnetisation circles with a single directly determined direction (Table 3).

In the remaining four sites (TEP5, TEP6, TEP8 and TEP11) in virtually all samples two more or less overlapped components were observed and, as mentioned for previous sites, both characteristic directions and remagnetisation circles were determined and used for calculation of the mean site direction (Fig. 7, Table 3).

Paleomagnetic results obtained on the 11 studied Pleistocene and Pliocene lava flows from the Tepeltitic area are shown in Table 3. As already discussed, only in four sites the mean site direction could be obtained from directly determined directions. In the seven remaining sites *ChRM* directions and remagnetisation circles were combined in order to calculate site means (*McFadden and McElhinny, 1988*). A problem with this method is that the finally calculated mean direction is biased towards the directly determined directions used for calculation. In order to confirm the reliability of the site means obtained in that way, in the cases in which we had applied the *McFadden and McElhinny (1988)* method for combination of directly determined directions and remagnetisation circles, we also calculated the mean obtained only from remagnetisation circles. Comparison of the site means obtained with both methods showed a good agreement in all cases, so that we could consider the mean directions obtained combining remagnetisation circles and directly determined directions shown in Table 3 as reliable.

When two specimens from the same core were demagnetised, if two directly determined directions were available, their mean was taken as the representative direction of that core. When both a direction and a remagnetisation circle from the same core had been determined, the former was used and the latter discarded. In the case of two remagnetisation circles from the same core, the one showing the lowest maximum angular

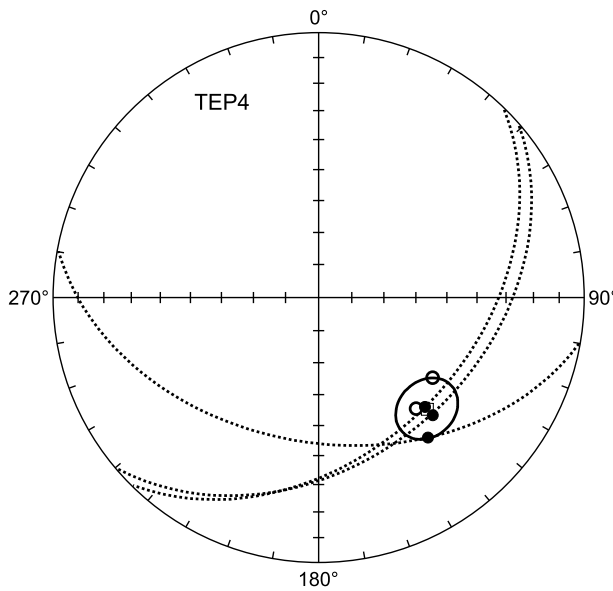

Fig. 7. Mean direction and α_{95} (after *McFadden and McElhinny, 1988*) for site TEP4. Solid dots - directions determined from great circles. Open dots - directly determined directions. Square - mean direction.

deviation (*MAD*) value was chosen. In one case (TEP5), however, we decided to include two remagnetisation circles from the same core in the calculation of the site mean, as both specimens had been demagnetised by different techniques and their demagnetisation paths were completely different.

As shown in Table 3 and Fig. 8, which display mean *ChRM* directions determined for each site, normal, reversed and intermediate polarities were obtained. A question to be posed is if these *ChRM* directions are primary paleodirections. Reversed and intermediate polarity directions determined in sites TEP1 TEP2, TEP3, TEP4, TEP6, TEP8 and TEP9 indicate that *ChRM* has been successfully isolated from normal present-day secondary directions. Analysis of hysteresis parameters (Figs 4 and 5) has shown, as discussed above, that in most sites a mixture of SD and MD grains is observed, so that at least part of the remanent magnetisation should be considered to be stable. In sites TEP4 and TEP8, however, the MD fraction is rather high. Nevertheless, in both cases an intermediate or reversed polarity direction could be determined, which shows an acceptably small scatter ($k = 86.1$ in TEP4 and $k = 36.2$ in TEP8). As will be discussed below, these polarities are not in disagreement with their $^{40}Ar/^{39}Ar$ ages.

5. RESULTS AND DISCUSSION

Plotting of the virtual geomagnetic pole (VGP) locations in the present geographical reference frame allows distinguishing between secular variation and intermediate polarity directions. Often a cut-off angle of 45° is adopted for VGP latitudes to discriminate between both regimes (e.g., *Johnson et al., 2008*; a detailed discussion on VGP cut-off angles can be found in *Camps et al., 2007*). VGPs obtained in the present study are shown in Table 2. Four sites yield normal polarity directions and, if the 45°-criterion is strictly applied, five provide reversed polarity and two yield intermediate polarity directions. Site TEP4, however, yields a VGP with a rather low latitude ($\phi_{VGP} = 49.3°$) which could also be considered transitional under the aforementioned criterion if VGP confidence limits *dp* (semi-axis of the ellipse of confidence along the site-to pole great circle) and *dm* (semi-axis perpendicular to the great circle) are taken into account, as $dp = 6.9°$ and $dm = 11.4°$. If the paleomagnetic pole obtained from the six Pliocene sites showing normal and reversed polarities (latitude $\phi = 81.1°$, longitude $\lambda = 94.3°$, $A_{95} = 7.3°$, $k = 74.9$) is compared with the 5 Ma window of the synthetic North American polar wander path from *Besse and Courtillot (2002)*, an angular difference of 9.4° is observed and although both A_{95} cones overlap, neither mean pole direction is contained within the A_{95} cone of the other mean. If the two Pleistocene sites with unambiguous normal or reversed polarity (leaving out site TEP4) are included in the mean, a paleomagnetic pole with longitude $\lambda = 131.6°$ and latitude $\phi = 80.0°$ ($k = 29.8$; $A_{95} = 10.3$) is obtained, angular differences of approximately 8° are observed with both the 0 Ma and the 5 Ma windows of the synthetic North American polar wander path from *Besse and Courtillot (2002)*. It might be concluded that the paleomagnetic pole obtained in the present study roughly agrees with the expected one, although a minor but significant difference cannot be completely ruled out.

If the mean paleomagnetic direction of the six Pliocene directions ($D = 357.4°$; $I = 23.1°$, $k = 41.8$; $\alpha_{95} = 10.5$) is compared with other Pliocene paleomagnetic directions obtained in the western sector of the TMVB (7 sites: $D = 3.5°$; $I = 33.1°$, $k = 23.8$; $\alpha_{95} = 12.6$; *Ruíz-Martínez et al., 2010*), an angle of 11° between both directions is observed (Fig. 8). The difference between both mean directions can be also expressed in terms of the difference between both declinations (rotation $R = D_6 - D_7$) and both inclinations (flattening $F = I_6 - I_7$). Indices 6 and 7 stand for the mean of six Pliocene directions obtained in the present study and the mean of seven Pliocene directions from the western sector of the TMVB, respectively. Values of $R = (-6 \pm 14)°$ and $F = (-10 \pm 13)°$ are obtained (confidence limits calculated after *Demarest, 1983*), indicating that no significant differences can be found between declinations and inclinations of both data sets. If both Pleistocene directions without site TEP4 are also included in the mean ($D = 353.4°$; $I = 27.2°$; $k = 25.4$; $\alpha_{95} = 11.2$), and the latter is compared with other Quaternary and Pliocene paleomagnetic directions obtained in the

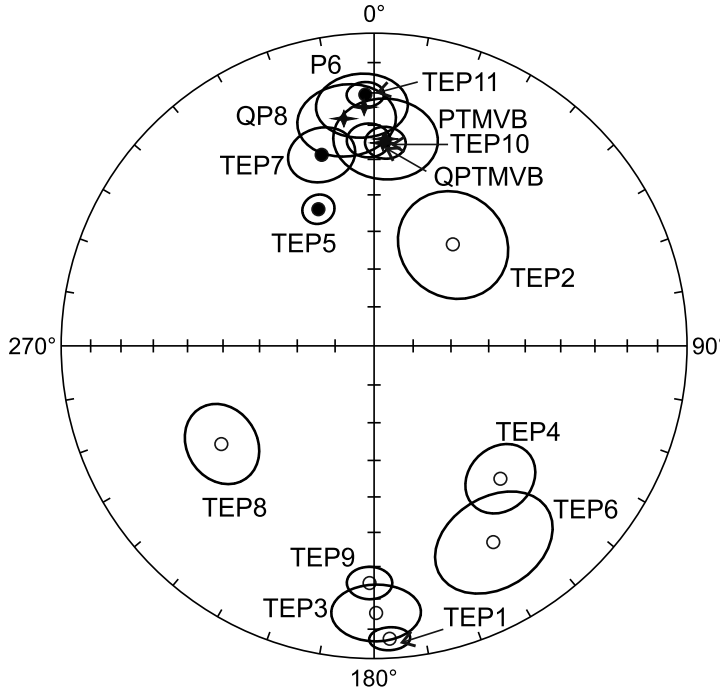

Fig. 8. Stereogram with mean directions and α_{95} confidence limits of of all studied sites. Solid dots - positive inclinations. Open dots - negative inclinations. P6 - six Pliocene directions. QP8 - six Pliocene and 2 Quaternary directions. PTMVB - other sites from the western sector of the Trans Mexican Volcanic Belt (*Ruiz-Martínez et al., 2010*). QPTMVB - mean Pliocene/Quaternary paleomagnetic direction of other sites from the western sector of the Trans Mexican Volcanic Belt (*Petronille et al., 2005*; *Rodríguez-Ceja et al., 2006*; *Ruiz-Martínez et al., 2010*). Mean directions of P6, QP8, PTMVB and QPTMVB are indicated by stars.

western sector of the TMVB (41 sites: $D = 358.8°$; $I = 33.9°$, $k = 18.8$; $\alpha_{95} = 5.3$; *Petronille et al., 2005*; *Rodríguez-Ceja et al., 2006*; *Ruíz-Martínez et al., 2010*) an angular deviation of 8º is recognised (Fig. 8). If the difference between both mean directions is again expressed in terms rotation R ($R = D_8 - D_{41}$) and flattening F ($F = I_8 - I_{41}$), a result of $R = (-5 \pm 11)°$ and $F = (-7 \pm 9)°$ is obtained (confidence limits calculated after *Demarest, 1983*), indicating that no significant differences can be found between declinations and inclinations of both data sets. Subindexes 8 and 41 stand for the mean of eight Pliocene and Pleistocene directions obtained in the present study and the mean of 41 Quaternary and Pliocene directions from the western sector of the TMVB, respectively. These results show that paleomagnetic directions from the present study basically agree with previous results obtained in the same study area from rocks of similar age, and do not indicate significant paleomagnetically detectable vertical-axis block rotations in the western TMVB area. It must be noted however, that the mean inclination of the Pliocene sites from the present study ($I = 23.1°$) seems to be shallower than the mean inclination of previously published Pliocene paleodirections from the western TMVB ($I = 33.1°$), although inclination uncertainties ΔI of both directions overlap.

As can be seen in Table 1, reverse-polarity sites TEP3, TEP9 and TEP1 have $^{40}Ar/^{39}Ar$ ages ranging between 3.87 and 4.01 Ma, and thus belong to the Gilbert chron (Fig. 9). The moderately older intermediate-polarity site TEP2 has an age of 4.32 ± 0.01 Ma, and can unambiguously be correlated with the normal-to-reversed Cochiti-Gilbert polarity transition (Fig. 9) at 4.30 Ma (*Ogg and Smith, 2004*). TEP8 also displays an intermediate polarity and its 3.54 ± 0.01 Ma age allows ascribing this site to the reversed-to-normal Gilbert-Gauss transition (Fig. 9) (3.58 Ma, *Lourens et al., 2004*). Normal-polarity sites TEP11, TEP10 and TEP7 yield ages between 2.91 and 3.40 Ma and belong to the Gauss chron (Fig. 9). Thus, the polarity observed in all these sites agrees well with the one expected from their radioisotopic age. The three remaining Quaternary sites have ages ranging between 220 and 542 ka, but only site TEP5 (307 ka) displays a normal polarity direction as expected for the Brunhes chron. Sites TEP4 and TEP6, however, are characterised by reversed or intermediate polarities.

Site TEP4 has an $^{40}Ar/^{39}Ar$ age of 542 ± 24 ka and displays a reversed or intermediate polarity magnetisation. The West Eifel volcanic field, once thought to record a single excursion (*Schnepp and Hradetzky, 1994*) has been shown to record five excursions between 730 and 530 ka B.P. (*Singer et al., 2006*). Specifically excursions West Eifel 4 and West Eifel 5 yield ages of 555 ± 4 ka and 528 ± 16 ka and thus, site TEP4 might record either the West Eifel 4 or the West Eifel 5 excursion.

Reversed polarity site TEP6 is however somewhat more difficult to correlate with a specific known excursion from the Brunhes chron. For this reason a test was performed on three different specimens of TEP6 to find out if self-reversal or partial self reversal could have happened in that site. All three specimens were initially AF demagnetised and partial thermal remanences (*pTRM*) were imparted to them at 250, 400 and 500°C. Magnetisation, which was measured after each remanence acquisition step, was observed to agree with the applied field direction.

The use of different names for excursions observed in different cores or lava flows combined with imprecise age control has sometimes led to some confusion in their labelling and correlation. Many studies have provided evidence for geomagnetic excursions in the 180–220 ka interval, but as fidelity and age control of available records has improved, evidence has accumulated for the occurrence of two excursions, Iceland Basin (188 ka) and Pringle Falls (211 ka) (see, for instance, *Laj and Channell, 2007*). *Shane et al. (1994)* found a geomagnetic excursion recorded in the Mamaku ignimbrite

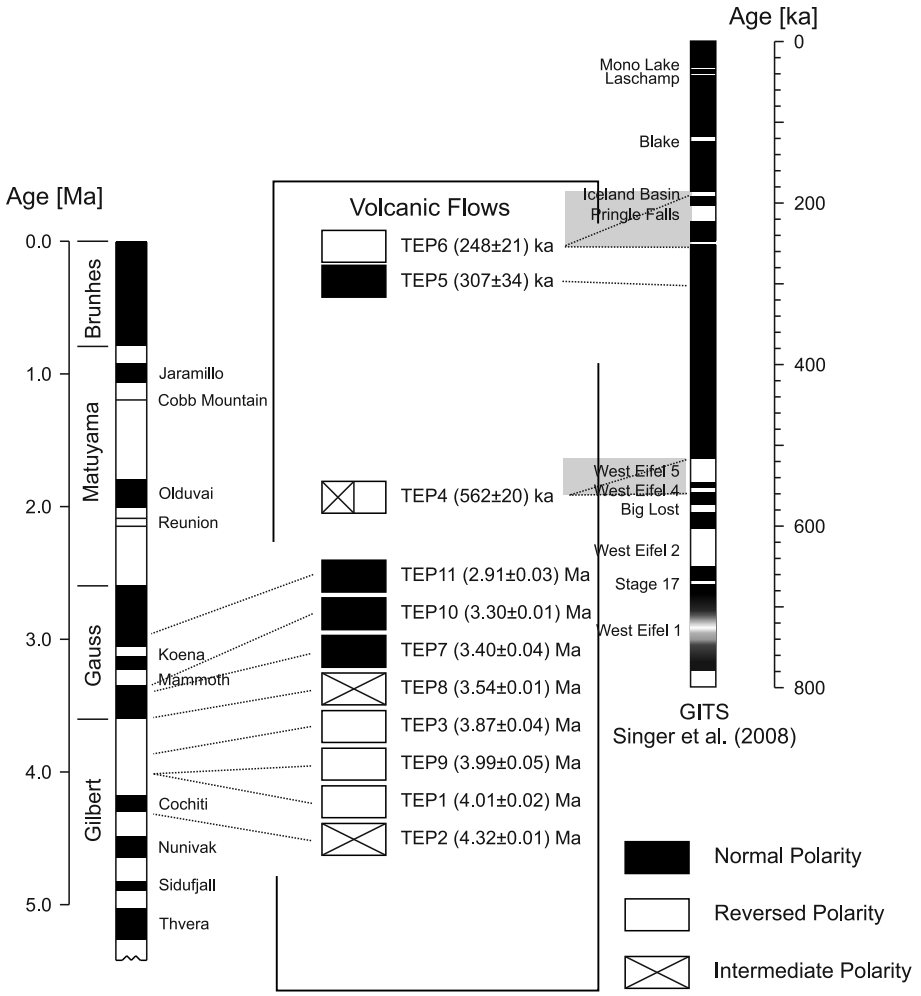

Fig. 9. Summary of results. $^{40}Ar/^{39}Ar$ ages and magnetic polarities of all studied sites are shown and compared with the Geomagnetic Polarity Time Scale (GPTS) for the last 5 Ma (left) and the Geomagnetic Instability Time Scale (right, *Singer et al., 2008*). Shaded areas at TEP4 and TEP6 reflect the age uncertainties of those sites, as they are the only ones in which no unambiguous correlation with the GITS can be performed (see text).

from the Taupo Volcanic zone in New Zealand, which they dated at 230 ± 12 ka by the isothermal plateau fission-track method. *Tanaka et al. (1996)* also conducted a paleomagnetic study in the Mamaku ignimbrite in parallel with detailed K/Ar and $^{40}Ar/^{30}Ar$ geochronology (*Houghton et al., 1995*). Three new $^{40}Ar/^{30}Ar$ ages yielded a mean of 0.22 ± 0.01 Ma for the Mamaku ignimbrite in which *Tanaka et al. (1996)* also observed transitional paleomagnetic directions, which they interpreted to correspond to the Pringle Falls excursion (*Herrero-Bervera et al., 1994*). *Oda et al. (2002)* redated an excursion from a core from Academian Ridge (Lake Baikal, Russia) previously inferred to record the Blake event obtaining a new age of 223 ka.

Thouveny et al. (2004; 2008) performed a paleomagnetic study in clayey-carbonate sequences deposited during the last 400 ka on the Portuguese margin. They found a marked relative paleointensity low associated with an anomalous declination swing at 240 ka B.P. and a minor cosmogenic nuclide production enhancement at 236 ka B.P., which they correlated with the excursion observed in the Mamaku ignimbrite (*Shane et al., 1994*; *Tanaka et al., 1996*). They also observed another slight but significant paleointensity low at 255 ka, validated by one single cosmogenic nuclide enhancement near the age of the Calabrian Ridge 0 (*Langereis et al., 1997*) and Fram Strait (*Nowaczyk and Bauman, 1992*) excursion.

Site TEP6 provides new evidence for a geomagnetic excursion around 220 ka B.P. The 220 ± 36 ka age observed in this site agrees well with the ages of the Pringle Falls excursion and the Mamaku record. However, coincidence with the Iceland Basin excursion (188 ka), or the excursions recorded in Calabrian Ridge 0 and Fram Strait cannot be completely excluded (Fig. 9).

Acknowledgements: This work was supported by project BU004A09 from Junta de Castilla y León (Spain). B.A. acknowledges the financial support given by UNAM-PAPIIT IN 113009. A.G. was supported by PAPIIT IN103311 and CONACYT N° 129653 and acknowledges the UNAM-DGAPA-PASPA, CONACYT and University of Burgos programs to facilitate sabbatical programs. A.C. acknowledges the funding obtained from the Spanish Ministry of Education (programa Campus de Excelencia Internacional). We wish to thank Augusto Rapalini and Pierre Camps for their useful comments and suggestions.

References

Alaniz-Álvarez S., Nieto-Samaniego A. and Ferrari L., 1998. Effects of strain rate in the distribution of monogenetic and pylogenetic volcanism in the Trans-Mexican Volcanic Belt. *Geology*, **26**, 591–594.

Besse J. and Courtillot V., 2002. Apparent and true polar wander and the geometry of the geomagnetic field over the last 200 Myr. *J. Geophys. Res.*, **107(B11)**, 2300, DOI: 10.1029/2000JB000050.

Camps P., Henry B., Nicolaysen K. and Plenier G., 2006. Statistical properties of paleomagnetic directions in Kerguelen lava flows: Implications for the late Oligocene paleomagnetic field. *J. Geophys. Res.*, **112**, B06102, DOI: 10.1029/2006JB004648.

Cande S.C. and Kent D.V., 1992a. A new geomagnetic polarity timescale for the late Cretaceous and Cenozoic. *J. Geophys. Res.*, **97**, 13917–13951.

Cande S.C. and Kent D.V., 1992b. Ultrahigh resolution marine magnetic anomaly profiles: A record of continuous paleointensity variations? *J. Geophys. Res.*, **97**, 15075–15083.

Day R., Fuller M. and Schmidt V.A., 1977. Hysteresis properties of titanomagnetites: grain-size and compositional dependence. *Phys. Earth. Planet. Inter.*, **13**, 260–267.

Demarest H., 1983. Error analysis for the determination of tectonic rotation from paleomagnetic data. *J. Geophys. Res.*, **88(B5)**, 4321–4328.

Dunlop D., 2002. Theory and application of the Day plot (M_{rs}/M_s versus H_{cr}/H_c). 1. Theoretical curves and tests using titanomagnetite data. *J. Geophys. Res*., **107(B3)**, DOI: 10.102972001JB000486.

Dunlop D. and Özdemir Ö., 1997. *Rock Magnetism: Fundamentals and Frontiers.* Cambridge University Press, Cambridge, U.K., 573 pp.

Fabian K., 2003. Some additional parameters to estimate domain state from isothermal magnetization measurements. *Earth Planet. Sci. Lett.*, **213**, 337–345.

Frey H., Lange R.A., Hall C.M., Delgado-Granados H. and Carmichael I.S.E., 2007. A Pliocene ignimbrite flare-up along the Tepic-Zacoalco rift: Evidence for the initial stages of rifting between the Jalisco block, Mexico) and North America. *GSA Bulletin*, **119(1/2)**, 49–64; DOI: 10.1130/B25950.

Grommé C.S., Wright T.L. and Peck D.L., 1969. Magnetic properties and oxidation of iron-titanium oxide minerals in Alae and Makaopuhi lava lakes, Hawaii. *J. Geophys. Res.*, **74**, 5277–5279.

Harland W.B., Armstrong R.L., Cox A.V., Craig L.E., Smith A.G. and Smith D.G., 1990. *A Geological Time Scale 1989*. Cambridge University Press, Cambridge, U.K., 263 pp.

Herrero-Bervera E., Helsley C.E., Sarna-Wojcicki A.M., Sarna-Wojcicki A.E., Lajoie K.R.,Meyer C.E., McWilliams M.O., Negrini R.N., Turrin B.D., Donnelly-Nolan J.M., and Liddicoat J.C., 1994. Age and correlation of a paleomagnetic episode in the western United States by $^{40}Ar/^{39}Ar$ dating and tephrochronology: The Jamaica, Blake or a new polarity episode? *J. Geophys. Res.*, **99**, 24091–24103.

Houghton B.F., Wilson C.J.N., McWilliams M.O., Lanphere M.A., Weaver S.D., Briggs R.M. and Pringle M.S., 1995. Chronology and dynamics of a large silicic magmatic system: central Taupo Volcanic Zone, New Zealand. *Geology*, **23**, 13–16.

Johnson C.L., Constable C.G., Tauxe L, Barendregt R.W., Brown L.L., Coe R.S., Layer P., Mejia V., Opdyke N.D.,Singer B.S., Staudigel H. and Stone D., 2008. Recent investigations of the 0-5 ma geomagnetic field recorded in lava flows. *Geochem. Geophys. Geosyst.*, **9**, Q04032, DOI: 10.1029/2007GC001696.

Kirschvink J.L., 1980. The least-square line and plane and the analysis of paleomagnetic data. *Geophys. J. R. Astron. Soc.*, **62**, 699–718.

Laj C. and Channell J.E.T., 2007. Geomagnetic excursions. In: Kono M. (Ed.), *Treatise in Geophysics*, **5**. Elsevier, Amsterdam, The Netherlands, 373–416.

Langereis C.G., Dekkers M.J., de Lange G.J., Paterne M. and van Saantvoort P.J.M., 1997. Magnetostratigraphy and astronomical calibration of the last 1.1 Myr from an eastern Mediterranean piston core dating of short events in the Brunhes. *Geophys. J. Int.*, **129**, 75–94.

Leonhardt R., 2006. Analyzing rock magnetic measurements; The RockMagAnalyzer 1.0 software. *Comput. Geosci.*, **32**, 1420–1431.

Lourens L., Hilgen N.J., Shackelton J., Lasker J. and Wilson J., 2004. Orbital tuning calibrations and conversions for the Neogene period. In: Gradstein F., Ogg J. and Smith A. (Eds.), *A Geologic Time Scale 2004*. Cambridge University Press, Cambridge, U.K., 469–471.

Lund S.P., Acton G.D., Clement B., Okada M. and Williams T., 2001. Brunhes chron magnetic field excursions recovered from Leg 172 sediments. In: Keigwin L.D., Rio D., Acton G.D. and Arnold E. (Eds.), *Proceedings of the ODP Science Research*, **172**, 1–18.

McFadden P.L. and McElhinny M.W., 1988. The combined analysis of remagnetisation circles and direct observations in paleomagnetism. *Earth Planet. Sci. Lett.*, **87**, 161–172.

Muttoni G., 1995. "Wasp-waisted" hysteresis loops from a pyrrothite and magnetite-bearing remagnetized Triassic limestone. *Geophys. Res. Lett*., **22**, 3167–3170.

Nowaczyk N.R. and Baumann M., 1992. Combined high-resolution magnetostratigraphy and nannofossil biostratigraphy for late Quaternary Artic ocean sediments. *Deep Sea Res.*, **39**, 567–601.

Oda H., Nakamura K., Ikehara K., Nakano T., Nishimura M. and Khlystov O., 2002. Paleomagnetic record from Academician ridge, Lake Baikal: A reversal excursion at the base of marine oxygen isotope stage 6. *Earth Planet. Sci. Lett.*, **202**, 117–132.

Ogg J.G. and Smith A.G., 2004. The Geomagnetic Polarity Time Scale. In: Gradstein F., Ogg J. and Smith A. (Eds.), *A Geologic Time Scale 2004*. Cambridge University Press, Cambridge, U.K., 63–86.

Pasquaré G., Garduño V.H., Tibaldi A. and Ferrari M., 1988. Stress pattern evolution in the Central Sector of the Mexican Volcanic Belt. *Tectonophysics*, **146**, 352–364.

Petronille M., Goguichaitchvili A., Henry B., Alva-Valdivia L.M., Rosas-Elguera J., Urrutia-Fucugauchi J., Rodríguez-Ceja M. and Calvo-Rathert M., 2005. Paleomagnetism of Ar-Ar dated lava flows from the Ceboruco-San Pedro volcanic field, western Mexico: Evidence for the Matuyama-Brunhes transition precursor and a fully reversed geomagnetic event in the Brunhes chron. *J. Geophys. Res.*, **110**, B08101, DOI: 10.1029/2004JB003321.

Petrovský E. and Kapička A., 2006. On determination of the Curie point from thermomagnetic curves. *J. Geophys. Res.*, **111**, B12S27, DOI: 10.1029/ 2006JB004507.

Prévot M., Mainkinen E.A., Grommé S. and Lecaille A., 1983. High paleointensity of the geomagnetic field from thermomagnetic studies on rift valley pillow basalts from the middle Atlantic ridge. *J. Geophys. Res.*, **88**, 2316–2326.

Roberts A., Yulong C. and Verosub K., 1995. Wasp-waisted hysteresis loops: mineral magnetic characteristics and discrimination of components in mixed magnetic systems. *J. Geophys. Res.*, **100(B9)**, 17909–17924.

Rodríguez-Ceja M., Goguitchaichvili A., Calvo-Rathert M., Morales-Contreras J., Alva-Valdivia L., Rosas-Elguera J., Urrutia-Fucugauchi J. and Delgado-Granados H., 2006. Paleomagnetism of the Pleistocene Tequila Volcanic field, Western Mexico. *Earth Planets Space*, **58**, 1349–1358.

Rosas-Elguera J., Aguilar Reyes B., Goguitchaichvili A., Rocha M., López Martínez M., Tostado-Plascencia M.M., Alva Valdivia L.M. and Caballero Miranda C., 2011. Paleomagnetic and rock-magnetic survey of eocene dike swarms from the Tecalitlan area (Western Mexico): Tectonic implications. *Stud. Geophys. Geod.*, **55**, 265–278.

Ruíz-Martínez V.C., Urrutia-Fucugauchi J. and Osete M.L., 2010. Paleomagentism of the Western and Central sectors of the Trans-Mexican volcanic Belt - implications for tectonic rotations and paleosecular variation in the past 11 Ma. *Geophys. J. Int.*, **180**, 577–595.

Schnepp E. and Hradetzky H., 1994. Combined paleointensity and $^{40}Ar/^{39}Ar$ age spectrum data from volcanic rocks of the West Eifel field, Germany: evidence for an early Brunhes geomagnetic excursion. *J. Geophys. Res.*, **99**, 9061–9076.

Shane P., Black T. and Westgate J., 1994. Isothermal plateau fission-track age for a paleomagnetic excursion in the Mamaku Ignimbrite, New Zealand, and implications for late Quaternary stratigraphy. *Geophys. Res. Lett.*, **21**, 1695–1698.

Singer B.S., Relle M.K. and Hoffman K.A., 2002. $^{40}Ar/^{39}Ar$ ages from transitionally magnetized lavas on La Palma, Canary Islands, and the geomagnetic instability timescale. *J. Geophys. Res.*, **107**, 2307, DOI: 10.1029/2001JB001613.

Singer B.S., Guillou H., Zhang X., Schnepp E. and Hoffman K.A., 2006. Multiple Brunhes chron excursions in the Eifel volcanic field. *EOS Trans. AGU*, **87(52)**, GP21A–GP1301.

Singer B.S., Jicha B.R., Kirby B.T., Geissman J.W. and Herrero-Bervera E., 2008. $^{40}Ar/^{39}Ar$ dating links Albuquerque Volcanoes to the Pringle Falls excursion and the Geomagnetic Instability Time Scale. *Earth Planet. Sci. Lett.*, **267**, 584–595.

Soffel H., 1975. Rock magnetism of the Monte Berici volcanites and age of volcanism deduced from the Heirtzler polarity time scale. *J. Geophys.*, **41**, 401–411.

Tanaka H., Turner G.M., Houghton B.F., Tachibana T., Kono M. and McWilliams M.O., 1996. Paleomagnetism and chronology of the central Taupo Volcanic zone, New Zealand. *Geophys. J. Int.*, **124**, 919–934.

Thouveny N., Carcaillet J., Moreno E., Leduc G. and Nérini D., 2004. Geomagnetic moment variation and paleomagnetic excursions since 400 kyr BP: a stacked record from sedimentary sequences of the Potuguese margin. *Earth Planet. Sci. Lett.*, **219**, 377–396.

Thouveny N., Bourlès D.L., Saracco G., Carcaillet J. and Bassinot F., 2008. Paleoclimatic context of geomagnetic dipole lows and excursions in the Brunhes, clue for an orbital influence on the geodynamo? *Earth Planet. Sci. Lett.*, **275**, 269–284.